Biochimica et Biophysica Acta 1817 (2012) 2027–2037

Contents lists available at SciVerse ScienceDirect

Biochimica et Biophysica Acta

journal homepage: www.elsevier.com/locate/bbabio

Composition of the mitochondrial electron transport chain in *Acanthamoeba castellanii*: Structural and evolutionary insights

Ryan M.R. Gawryluk [a], Kenneth A. Chisholm [b], Devanand M. Pinto [b], Michael W. Gray [a,*]

[a] Centre for Comparative Genomics and Evolutionary Bioinformatics, Department of Biochemistry and Molecular Biology, Dalhousie University, Halifax, Nova Scotia, Canada
[b] Institute for Marine Biosciences, National Research Council of Canada, Halifax, Nova Scotia, Canada

ARTICLE INFO

Article history:
Received 5 April 2012
Received in revised form 6 June 2012
Accepted 8 June 2012
Available online 15 June 2012

Keywords:
Mitochondrion
Protist
Electron transport chain
Mass spectrometry

ABSTRACT

The mitochondrion, derived in evolution from an α-proteobacterial progenitor, plays a key metabolic role in eukaryotes. Mitochondria house the electron transport chain (ETC) that couples oxidation of organic substrates and electron transfer to proton pumping and synthesis of ATP. The ETC comprises several multiprotein enzyme complexes, all of which have counterparts in bacteria. However, mitochondrial ETC assemblies from animals, plants and fungi are generally more complex than their bacterial counterparts, with a number of 'supernumerary' subunits appearing early in eukaryotic evolution. Little is known, however, about the ETC of unicellular eukaryotes (protists), which are key to understanding the evolution of mitochondria and the ETC. We present an analysis of the ETC proteome from *Acanthamoeba castellanii*, an ecologically, medically and evolutionarily important member of Amoebozoa (sister to Opisthokonta). Data obtained from tandem mass spectrometric (MS/MS) analyses of purified mitochondria as well as ETC complexes isolated via blue native polyacrylamide gel electrophoresis are combined with the results of bioinformatic queries of sequence databases. Our bioinformatic analyses have identified most of the ETC subunits found in other eukaryotes, confirming and extending previous observations. The assignment of proteins as ETC subunits by MS/MS provides important insights into the primary structures of ETC proteins and makes possible, through the use of sensitive profile-based similarity searches, the identification of novel constituents of the ETC along with the annotation of highly divergent but phylogenetically conserved ETC subunits.

1. Introduction

Mitochondria are eukaryotic organelles derived in evolution via an endosymbiotic association between an α-proteobacterium and a host cell of still-debated origin [1–3]. Although many diverse and essential cellular functions are associated with mitochondria, including iron–sulfur (Fe–S) cluster biosynthesis and the metabolism of amino acids and fatty acids, these organelles are best known for the vital role they play in cellular energy generation, primarily through coupled oxidative phosphorylation [4]. Under aerobic conditions, pyruvate is decarboxylated in mitochondria via the pyruvate dehydrogenase multienzyme complex and passed as acetyl-CoA into the tricarboxylic acid (TCA) cycle. Reducing equivalents in the form of NADH are generated via the TCA cycle, among other pathways, and subsequently oxidized by the electron transport chain (ETC): a series of multiprotein enzyme complexes (CI–CIV) that, with the exception of CII, couple the energy derived from electron transfer to the translocation of protons from the mitochondrial matrix into the intermembrane space. The resulting electrochemical gradient is exploited by the F_1F_o ATP synthase (CV) for the synthesis of adenosine triphosphate (ATP).

All complexes of the mitochondrial ETC as well as CV were present in the eubacterial progenitor of mitochondria; many proteins specified by mitochondrial DNA (mtDNA) are subunits of the ETC, and at least one subunit of each complex is encoded by mtDNA in diverse eukaryotes [5]. In contrast, mitochondrial ETC complexes studied to date are markedly larger and more intricate than their bacterial antecedents, as they have accrued a number of subunits not present in bacteria [6–8]. Some subunits, which are present across the domain Eucarya, arose prior to the diversification of modern eukaryotic supergroups, whereas others are suggested to be lineage-specific additions [7].

The composition of the ETC has been analyzed comprehensively in relatively few systems, notably some animals, fungi, plants/green algae and parasitic trypanosomes [9–17]. However, data concerning the makeup of the ETC in unicellular eukaryotes (protists) are currently very limited. Protists account for most of the evolutionary and biochemical diversity within the eukaryotic domain; for this reason, cataloging the composition of the mitochondrial ETC in free-living protists is critical to our understanding of the function and evolution of the ETC in general. For instance, characterization of ETC composition in protists will undoubtedly facilitate comparison of individual ETC complexes across eukaryotes and provide clues as to when various subunits arose in

* Corresponding author at: Room 8F-2, Department of Biochemistry and Molecular Biology, Dalhousie University, 5850 College Street, Halifax, Nova Scotia, Canada B3H 4R2. Tel.: +1 902 494 2521.
E-mail address: m.w.gray@dal.ca (M.W. Gray).

0005-2728/$ – see front matter © 2012 Elsevier B.V. All rights reserved.
doi:10.1016/j.bbabio.2012.06.005

evolution. Further, identification of homologs of divergent ETC subunits in protists may allow recognition of previously unappreciated homologies with ETC subunits in other lineages (animals, fungi and plants), effectively by bridging the sequence similarity gap [7,18]. Lastly, direct characterization of protist ETC complexes facilitates the discovery of novel subunits, providing a functional context for certain hypothetical proteins identified in genomic or proteomic studies [19].

As a result of recent advances in genome and transcriptome sequencing, investigations of protist mitochondrial ETC proteomes have become more feasible and wide-ranging. The extensive sequence databases permit bioinformatic analyses aimed at mapping subunit presence and absence across the breadth of eukaryotes. Importantly, the direct identification of proteins comprising mitochondrial and ETC proteomes via tandem mass spectrometry (MS/MS) is dependent on the availability of comprehensive sequence databases. Many mitochondrial proteins, including ETC proteins, are not confidently assigned as such via sequence similarity searches or mitochondrial localization algorithms [20,21], and because the presence of a gene in a genome does not guarantee its expression, it is imperative to augment bioinformatic analyses with proteomic analysis of whole mitochondria and isolated ETC complexes to more fully and accurately define ETC composition.

We have undertaken an inventory of ETC proteins from the amoeboid protist *Acanthamoeba castellanii* (supergroup Amoebozoa), a ubiquitous and evolutionarily important soil and freshwater amoeba for which mitochondrial genomic and extensive nuclear genomic/transcriptomic data are publicly available (NC_001637.1; http://www.hgsc.bcm.tmc.edu/microbial-detail.xsp?project_id=163). We have employed blue native polyacrylamide gel electrophoresis (BN-PAGE) [22] to isolate ETC complexes from purified mitochondria and have investigated the composition of individual complexes using MS/MS. Where classical ETC proteins were not directly identified from BN-PAGE-isolated complexes via MS/MS, we interrogated a database generated from an ongoing proteomic inventory of whole *A. castellanii* mitochondria as well as available sequence databases using standard (e.g., BLAST) and profile (e.g., HMMER, PSI-BLAST) similarity searches.

2. Materials and methods

2.1. Growth of A. castellanii and purification of mitochondria

Cells and mitochondria of *A. castellanii* (strain Neff, ATCC 30010) were prepared essentially as in [23] except that: (a) cells were not washed with phosphate-buffered saline prior to lysis, (b) the crude mitochondrial pellet was washed only once with mitochondrial wash buffer in order to preserve mitochondrial integrity, (c) BSA was omitted from step-sucrose gradient buffers, and (d) mitochondria used for whole proteome analysis, but not BN-PAGE, were purified on two successive step sucrose gradients.

2.2. BN-PAGE for isolation of ETC complexes

BN-PAGE of whole *A. castellanii* mitochondria was carried out as described previously [24] in either 3.5–12%, 4–12% or 4–15% polyacrylamide gels. Molecular weights of ETC complexes were estimated using the NativeMark unstained protein standard (Invitrogen).

2.3. Linear sucrose gradient centrifugation of mitochondrial protein complexes

Linear sucrose gradients were performed as in [25], except that (a) mitochondria were resuspended in BN-PAGE isolation buffer [22] and solubilized on ice by the addition *n*-dodecyl-β-D-maltoside (DDM) dissolved in BN-PAGE isolation buffer (final detergent:protein ratio of 2:1) and (b) the linear sucrose gradient (10–40% sucrose, w:v) was made in a buffer containing 75 mM 6-aminocaproic acid, 50 mM bis–tris (pH 7.0), 1 mM phenylmethanesulfonylfluoride (PMSF), and 0.1 mg/ml DDM.

2.4. In-gel enzyme activity assays

All in-gel enzyme activity assays were carried out overnight, at room temperature, immediately after BN-PAGE experiments, essentially according to [26].

2.5. Lysis of whole mitochondria and enrichment for soluble and membrane fractions for MS/MS

Two milligrams of whole mitochondria were resuspended to a final volume of 2 ml in a solution containing 50 mM Tris·HCl, pH 7.6, 1 mM Na_2EDTA and 1 mM PMSF. Mitochondria were passed twice through a French press at 10,000 psi and the lysate was centrifuged at 33,000 rpm (RCF_{avg} of ~70,000×*g*) for 1 h at 4 °C in a Beckman Type 75 Ti rotor. The resulting pellet (membrane-protein-enriched fraction, MPE) was washed with buffer, re-sedimented and stored at −70 °C. Proteins contained in the supernatant (dilute soluble-protein-enriched fraction, SPE) were precipitated with trichloroacetic acid/acetone [27].

2.6. SDS polyacrylamide gel electrophoresis (SDS-PAGE) and excision of bands for MS/MS

Approximately 40 μg of protein was separated on an 8×7.3 cm gel (Bio-Rad Mini-Protean II system) with an ~0.5 cm 4% stacking gel and a 9–15% linear acrylamide gradient resolving gel at 15 mA constant, according to [28]. The lanes from the Coomassie Blue R250-stained gel were excised into approximately equal-sized bands (19 bands from the SPE fraction, 22 from the MPE fraction and 24 from the whole mitochondrial fraction) for MS/MS analysis.

2.7. Mass spectrometry

2.7.1. In-gel protein digest

Excised protein bands (either SDS-PAGE or BN-PAGE) were digested manually or with a Genomic Solutions Progest automated system as described in [24].

2.7.2. In-solution protein digest of whole mitochondria

A sample containing approximately 500 μg of mitochondrial protein was diluted to a concentration of 1 mg/ml in 50 mM ammonium bicarbonate, pH 8.0 (AB) with protease inhibitor (Set III, Calbiochem 539134). In-solution protein digestion was carried out as in [29], except that an acid-labile surfactant (Rapigest, Waters 186001861) was added at a concentration of 0.1% (w/v) to improve solubilization and protein digestion (used according to manufacturer's specifications).

2.7.3. SCX-HPLC of tryptic peptides derived from whole mitochondria

Five hundred micrograms of tryptic peptides were fractionated by SCX-HPLC into 45 fractions as in [29].

2.7.4. MS/MS and protein identification (all samples)

Reversed-phase LC–MS/MS (RP-HPLC) sample analysis, data acquisition and Mascot searches were performed as in [24]. Data files were searched against: (1) a 6-frame translation of a CAP3-clustered EST database, consisting of ESTs generated by random 454 sequencing and through TBestDB [30]; (2) a set of previously predicted *A. castellanii* mtDNA-encoded proteins [31]; (3) a 6-frame translation of the complete *A. castellanii* mitochondrial genome sequence [31]; and (4) an in-house predicted set of nuclear DNA (nuDNA)-encoded proteins (preliminary gene predictions; PGPs), generated by Augustus [32] from a draft version of the *A. castellanii* nuclear genome sequence. For nuDNA-encoded proteins predicted from either EST or PGP datasets and identified in the BN-PAGE and whole mitochondria proteome analyses, only

those containing one or more peptides with ion scores ≥38 (exceeding the Mascot 95% significance threshold) were considered. Typically, proteins from the PGP dataset were only considered if they were poorly represented in the EST dataset (in order to offset the biases associated with using an expression-based database alone). In the case of mtDNA-encoded proteins, certain peptides below this threshold were accepted after manual inspection. In order to assess the false positive rates for peptide identifications in the 6-frame translated EST dataset, we used the built-in Mascot feature that queries random protein sequences matched in length and amino acid composition to the entries in the database.

In sum, four different strategies were used in the MS/MS-based analysis of *A. castellanii* mitochondria (aside from MS/MS after BN-PAGE): (1) LC/LC–MS/MS analysis of whole mitochondria (WM), (2) 1D SDS-PAGE/LC–MS/MS analysis of whole mitochondria (SWM), (3) 1D SDS-PAGE/LC–MS/MS analysis of SPE fractions and (4) 1D SDS-PAGE/LC–MS/MS analysis of MPE fractions.

2.8. Methods for inference of homology

Annotation of proteins identified by MS/MS analysis was performed by querying a variety of databases [30,33] using BLAST [34] (BLASTp, tBLASTn and PSI-BLAST algorithms). Alignments were inspected manually.

In order to identify certain proteins expected to be found in *A. castellanii* but not easily uncovered by standard homology searches, HMMER 3.0 searches [35] of a 6-frame translation of the *A. castellanii* EST dataset or the mitochondrial proteome dataset were performed. In combination, we considered: (1) the E-value and rank of the putative homolog when queried with a profile HMM (all putative homologs ranked among the top 3 when the mitochondrial proteome dataset was queried with the profile HMM; expect (E-) values were relatively high, though most were ≤0.05); (2) whether the highest ranking result was identified via MS/MS as a component of a protein complex (e.g., if a putative CI subunit was being searched for, was the top HMMER match an established component of CI?); and (3) the size and physicochemical properties of the protein in question in relation to authentic homologs.

2.9. Analysis of semitryptic peptides

A Mascot semitryptic peptide search was employed to detect the mature N-terminus of Cox2, along with an internal Atpa peptide, essentially as described in [36].

2.10. Phylogeny of Core1/MPPβ proteins

Maximum likelihood trees were reconstructed from hand-edited alignments with RAxML-HPC [37] under the WAG + Γ model (using the PROTGAMMAWAGF option) with 25 categories of substitution rate variation. One hundred bootstrap replicates were performed as a measure of statistical support for inferred nodes.

3. Results and discussion

3.1. Complex I (NADH:ubiquinone oxidoreductase; CI)

E. coli CI consists of 14 subunits (Nad1–Nad11 and Nad4L along with 24-kDa and 51-kDa subunits); however, the corresponding α-proteobacterial complex has 17 subunits, including three additional proteins (B17.2, AQDQ and 13-kDa) that were previously believed to be specific to mitochondrial CI [38]. To simplify comparisons with other publications, we refer here to the 'traditional' 14-subunit bacterial core. In contrast, mitochondrial CI has accrued 'supernumerary' subunits [7,8], e.g., 31 in bovine CI [9] and 35 in *A. thaliana* CI [25], for a total of 45 and 49 subunits, respectively. At least 19 of the supernumerary subunits were acquired early in eukaryotic evolution, although others appear to have evolved within particular eukaryotic lineages [7]. More recent bioinformatic analyses, employing profile-based queries and a broader phylogenetic sampling, suggest that CI from the last eukaryotic common ancestor contained at least 40 subunits, and that the number of lineage-specific CI additions is in fact small [18].

3.1.1. Size and higher order structure of *A. castellanii* CI

Enzymatically active CI was detected by BN-PAGE as an ~940-kDa complex (Fig. 1), while an inactive ~820-kDa variant was identified by comparison to the staining profile of active CI following parallel 2D BN/SDS-PAGE of the two complexes [24]. The estimated size for monomeric CI is consistent with the size reported for CI from a variety of other eukaryotes, including a prior investigation of *A. castellanii* CI [39]. The active CI band stained faintly with Coomassie Blue relative to neighboring bands, such as dimeric CV (discussed below), whereas the 820-kDa variant co-migrates with other complexes. As a result, comprehensive proteomic detection of subunits from isolated CI has proven difficult, although all prokaryotic and eukaryotic core subunits were identified through a combination of BN-PAGE and detailed bioinformatic searches of proteins identified in proteome analysis of whole mitochondria and/or relevant *A. castellanii* sequence databases.

3.1.2. Detection of CI subunits via BN-PAGE-MS/MS

Proteomic analyses of the 940- and 820-kDa CI variants revealed a similar array of subunits, although more proteins were identified in the 820-kDa complex, likely due to its higher apparent abundance (see Supplemental File 1A-1). Differences included detection of the 51-kDa subunit in the 940-kDa band but not the 820-kDa one, a finding in agreement with in-gel enzyme activity assays, as the 51-kDa subunit forms part of the N module of CI that is responsible for oxidation of NADH [8]. In addition to subunits of the membrane and peripheral domains, we also detected two homologs of γ-type carbonic anhydrases in both CI variants, as described elsewhere [24].

Of the 19 putative supernumerary subunits added to CI early in eukaryotic evolution [7], we found 17 in one or both of the 940- and 820-kDa complexes (only AQDQ and the 13-kDa subunit were not detected) and 8 in both complexes (Table 1). Similarly, we identified bioinformatically putative homologs of 29 of the 32 eukaryote-specific CI proteins proposed by Cardol [18]; 27 of these proteins were detected via MS/MS of whole mitochondria, whereas 25 were identified in one or both of the CI variants. Interestingly, among these identified subunits is SDAP (acyl-carrier protein)—an experimentally validated component of CI in animals and fungi, but a soluble matrix protein in plants [40]. This subunit was also present in a CI-enriched BN-PAGE band from the ciliated protozoon *T. thermophila* (RMRG, unpublished results). Together, these results suggest that SDAP is an ancestral component of mitochondrial CI that may have been lost from CI in the plant lineage. Also, we detected a homolog of the B14.7 subunit, which in turn is homologous to members of the Tim17/Tim22/Tim23 protein import family. An unambiguous orthologous relationship of the *A. castellanii* protein to B14.7 (vs. Tim17/Tim22/Tim23) could not be established from the sequence alone; however, detection of this protein in both CI variants argues strongly that it is B14.7.

Two putative CI subunits identified by proteomic analysis in both the 940- and 820-kDa complexes, but with no apparent BLASTp homologs, were annotated following HMMER profile searches as the eukaryotic CI subunits MWFE and ASHI: small proteins associated with the membrane arm of CI, each containing a single predicted transmembrane helix [8]. Notably, the MWFE and ASHI subunits in another amoebozoon, *Dictyostelium discoideum*, are each more similar to other eukaryotic homologs than are the corresponding *A. castellanii* proteins. MWFE and ASHI are conserved across Eucarya, although ASHI was initially considered to be limited to animals and fungi [7], and are experimentally verified components of CI in animals [9], fungi [10] and plants [25].

Our BN-PAGE analyses have uncovered homologs of several CI subunits (B14.5b, B15 and NUUM [41]) that were recently identified

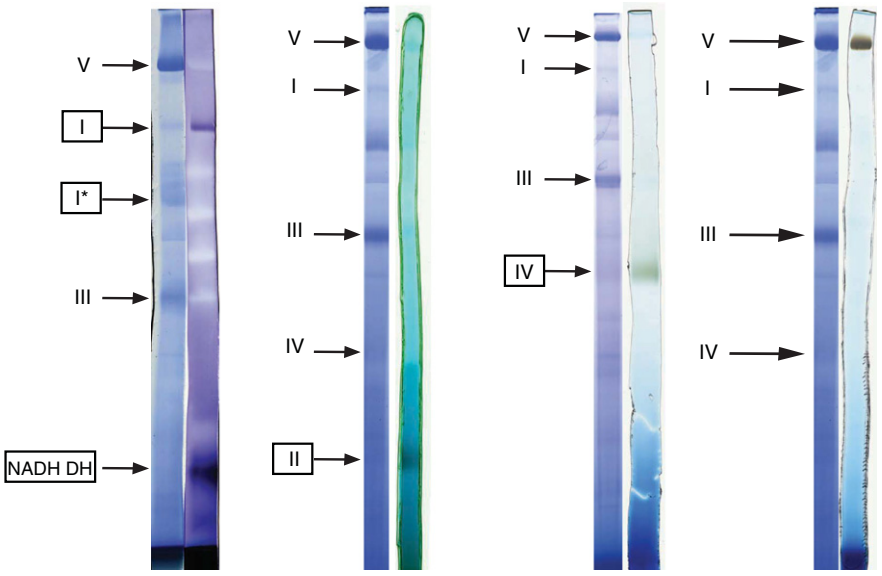

Fig. 1. BN-PAGE profiles and in-gel activity assays of *A. castellanii* ETC complexes. Gel strips from BN-PAGE experiments stained with either Coomassie Blue R250 (left) or enzyme activity stain (right) for each complex are shown. The relevant ETC complex name in each case is demarcated with a box. No specific CIII activity stain is available, so CIII is indicated only by an arrow in Coomassie Blue R250-stained gels. Profiles are not identical as not all gels consisted of the same acrylamide gradient.

bioinformatically in the amoebozoon, *D. discoideum*, along with putative homologs of subunits B9 and B14.5a, which were not identified in *D. discoideum* [18].

3.1.3. CI subunits detected via proteome analysis of whole mitochondria and/or bioinformatic searches

Although difficulties in obtaining large quantities of BN-PAGE-purified CI have precluded an exhaustive, direct proteomic analysis of the enzyme complex, homology searches of the *A. castellanii* mitochondrial proteome and EST datasets have identified most of the classical CI subunits. Importantly, 19/19 proposed eukaryotic core CI subunits and 12/14 prokaryotic core CI subunits (Nad2 and Nad4L were not detected) were identified by proteomic analysis of whole mitochondria (Table 1, Supplemental File 1B-1). Among the proteins identified in whole mitochondria but not in BN-PAGE-isolated CI are the 24-kDa subunit (NADH-oxidizing domain), AQDQ and Nad6.

Bioinformatic analyses revealed two putative CI subunits not detected by proteomic analysis: AGGG and MLRQ. The *A. castellanii* AGGG homolog was readily identifiable using the human homolog as BLAST query, whereas an MLRQ homolog from the amoebozoon *Polysphondylium pallidum* was used to retrieve an ~10-kDa MLRQ homolog (*D. discoideum* and *P. pallidum* homologs are more conserved than the *A. castellanii* counterpart, so that queries using the animal MLRQ sequences do not retrieve the putative *A. castellanii* MLRQ). Both of these proteins have homologs in multiple eukaryotic groups. In combination with the results presented above and other recent findings [24], these results suggest that the ancestral eukaryotic CI may have been even larger than previously believed (≥39–40 subunits), in good agreement with another recent analysis [18].

In comparison with amoebozoan relatives (*D. discoideum*, in particular), it appears that in general the same subunits of CI are conserved. Apart from the ESSS, B9 and B14.5a subunits, all CI constituents found in *A. castellanii* can be identified bioinformatically in *D. discoideum*. Notably, however, *A. castellanii* and *D. discoideum* CI orthologs are generally no more similar to each other than each is to its non-amoebozoan CI counterparts.

3.1.4. CI assembly proteins

Our proteomic analysis has revealed a number of characterized CI assembly factors [42] (Supplemental File 1B-1), including homologs of Ind1, a P-loop NTPase specifically required for assembly of CI Fe–S clusters, C8orf38 and C20orf7. Conversely, proteomic analysis failed to detect Cia30/NDUFAF1, NDUFAF3, FOXRED1, B17.2L and MidA, all of which are nuDNA-encoded in *A. castellanii* (Supplemental File 1C-1). No established CI assembly factors were identified by proteomic analyses of BN-PAGE-isolated CI.

3.2. Complex II (succinate:ubiquinone oxidoreductase; CII) in *A. castellanii*

Structurally, CII is the simplest of the ETC complexes, composed of only 4 subunits in bacteria, animals and fungi, although 8 subunits have been reported in plants [13] and 12 in trypanosomes, including a split SdhB [17,43].

We found enzymatically active *A. castellanii* CII to be ~130 kDa (Fig. 1), consistent with the size of CII in other eukaryotes. Proteomic analyses of BN-PAGE-isolated CII detected the 4 classical subunits of CII (SdhA–D), all of which are nuDNA-encoded in *A. castellanii* (Table 2, Supplemental File 1A-2). No *A. castellanii*-specific CII proteins were identified in this analysis; however, a large number of high abundance, non-CII mitochondrial proteins were detected in this sample (Supplemental File 1A-2). This result is likely attributable to the physical size of CII, as smaller protein complexes are more prone to contamination in such experiments by co-migrating protein multimers. As a result, it is possible that novel CII-specific proteins might be obscured in these proteomic analyses by other abundant, non-CII mitochondrial proteins. Nonetheless, the small size of *A. castellanii* CII suggests that few if any proteins were missed, as the combined estimated molecular weights of SdhA–D are in agreement with molecular weight estimates of the complex as a whole.

While *sdhA*, *sdhC* and *sdhD* appear to be single-copy genes in *A. castellanii*, two *sdhB* loci encode distinct isoforms of SdhB. Only one SdhB variant was detected in BN-PAGE-enriched CII or in whole mitochondria (Supplemental File 1C-2). EST coverage of the undetected isoform is not extensive; hence, it is not clear whether this variant is a constitutively expressed but minor isoform present at all times, or whether it is required only under certain conditions.

3.3. Complex III (ubiquinol:cytochrome *c* oxidoreductase; CIII)

In bacteria, CIII comprises 3 subunits—cytochrome *b* (Cob), the Rieske Fe–S protein (Isp) and cytochrome *c*1 (CytC1). Mitochondrial

Table 1
A. castellanii CI subunits and CI assembly proteins.

Protein	Genome	Sector	WM	940	820	Euk.	Bact.	Amoeb.
CI subunits								
Nad1	M	Iγ	+	–	+	+	+	+
Nad2	M	Iγ/ Iβ	–	–	–	+	+	+
Nad3	M	Iγ/ Iβ	+	–	+	+	+	+
Nad4	M	Iβ	+	–	+	+	+	+
Nad4L	M	Iγ/ Iβ	–	–	–	+	+	+
Nad5	M	Iβ	+	–	+	+	+	+
Nad6	M	Iγ/ Iβ	+	–	–	+	+	+
Nad7	M	Iλ	+	+	+	+	+	+
Nad8	N	Iλ	+	+	+	+	+	+
Nad9	M	Iλ	+	+	+	+	+	+
Nad10	N	Iλ	+	+	+	+	+	+
Nad11	M	Iλ	+	+	+	+	+	+
24-kDa	N	FP	+	–	–	+	+	+
51-kDa	N	FP	+	+	–	+	+	+
39-kDa	N	Iγ	+	+	+	+	+[a]	+
B14.7	N	Iλ	+	+	+	+	–	+[c]
15-kDa	N	Iγ	+	–	+	+	–	+
13-kDa	N	Iλ	+	–	–	+	+[b]	+
AQDQ	N	Iλ	+	–	–	+	+[b]	+
ESSS	N	Iβ	+	–	+	+	–	–
MWFE[d]	N	Iγ	+	+	+	+	–	+
PDSW	N	Iβ	+	–	+	+	–	+
PGIV	N	Iγ	+	+	+	+	–	+
SDAP	N	Iγ/Iβ	+	+	+	+	+[a]	+
B22	N	Iβ	+	+	+	+	-	+
B18	N	Iβ	+	–	+	+	-	+
B17.2	N	Iλ	+	+	–	+	+[b]	+
B16.6	N	Iλ	+	–	+	+	–	+
B14	N	Iγ	+	+	–	+	–	+
B13	N	Iλ	+	+	+	+	–	+
B12	N	Iβ	+	+	+	+	–	+
B8	N	Iλ	+	+	–	+	–	+
AcCa1	N	CA	+	+	+	+	+[a]	+
AcCa2	N	CA	+	+	+	+	+[a]	+
ASHI[d]	N	Iβ	+	+	+	+	–	+
B15	N	Iγ/Iβ	+	+	+	+	–	+
AGGG	N	Iβ	–	–	–	+	–	+
B14.5b[d]	N	Iβ	+	+	+	+	–	+
20.9	N	Iγ/Iβ	+	+	+	+	–	+
NUUM	N	?	–	+	–	+	–	+
B14.5a[d]	N	Iλ	+	+	–	+	–	–
B9[d]	N	Iγ	–	–	+	+	–	–
MLRQ	N	Iγ/Iβ	–	–	–	+	–	+
CI assembly proteins								
Ind1	N	n/a	+	–	–	+	+	+
C8orf38	N	n/a	+	–	–	+	+	+
C20orf7	N	n/a	+	–	–	+	+	+
MidA	N	n/a	–	–	–	+	+	+
Ndufaf1	N	n/a	–	–	–	+	+	+
Ndufaf3	N	n/a	–	–	–	+	+	+
Foxred1	N	n/a	–	–	–	+	+	-
B17.2L	N	n/a	–	–	–	+	-	+

Proteins identified via a combination of BN-PAGE proteomic analysis of the 940- ("940") and 820-kDa ("820") CI isoforms, as well as proteomic analyses of whole mitochondria ("WM") are reported. The sequences of all listed proteins can be retrieved through bioinformatic searches of *A. castellanii* sequence databases. Whether the protein in question is present in other eukaryotes ("Euk."), bacteria ("Bact.") and/or other amoebozoons ("Amoeb.") is also indicated (+ sign and gray shading). The genome in which a given protein is encoded is noted (N; nuclear, M; mitochondrial). Protein sequences for all entries, including delineation of identified peptides, are available in Supplemental File 1.
[a]These proteins have bacterial homologs but are not known to be components of CI in bacteria.
[b]These proteins have bacterial homologs and are known to be CI components in α-proteobacteria [38].
[c]Other amoebozoan species likely have B14.7 homologs (member of Tim17/Tim22/Tim23 family) but definitive orthologs could not be established on the basis of similarity searches alone.
[d]These subunits were annotated via HMMER 3.0 profile searches.

Table 2
A. castellanii CII subunits.

Protein	Genome	WM	BN	Euk	Bact.	Amoeb.
SdhA	N	+	+	+	+	+
SdhB-1	N	+	+	+	+	+
SdhB-2	N	–	–	+	+	+
SdhC	N	+	+	+	+	+
SdhD	N	+	+	+	+	+

See Table 1 for details. Protein sequences for all entries, including delineation of identified peptides, are available in Supplemental File 1. BN, proteomic analysis of complex isolated by BN-PAGE.

CIII is more complex, typically containing a well-conserved set of 6–7 supernumerary subunits that are not directly involved in electron transfer [44], including the large 'core' proteins, Core1 and Core2, which project into the mitochondrial matrix, and a collection of smaller, eukaryote-specific proteins (Qcr6–Qcr10). In all CIII-containing eukaryotes studied to date, Cob is mtDNA-encoded, whereas the other subunits are encoded in the nucleus.

3.3.1. Size and higher order structure of *A. castellanii* CIII

A. castellanii CIII migrated in BN-PAGE as an ~550 kDa complex (Fig. 1), the typical size of eukaryotic CIII. Thus, CIII likely exists as a stable homodimer in *A. castellanii*, as it does in other eukaryotes and prokaryotes [45].

3.3.2. Composition of CIII

Initial bioinformatic searches retrieved all expected proteins except Qcr10, the least well-conserved of the Qcr proteins. Proteomic analysis of BN-PAGE-isolated CIII detected all of the subunits identified bioinformatically (Supplemental File 1A-3), and additionally revealed a predicted 10.7-kDa protein that retrieves the human homolog of Qcr10 in BLASTp. Although the *A. castellanii* Qcr10 candidate is slightly larger than Qcr10 homologs from other eukaryotes (8.6 kDa and 6.5 kDa in yeast and bovine mitochondria, respectively), a multiple protein alignment (not shown) and profile similarity search using authentic Qcr10 homologs suggest that the 10.7-kDa protein is a bona fide Qcr10 homolog. All 10 CIII subunits were detected in our proteomic analysis of whole mitochondria (Table 3, Supplemental File 1B-3). In sum, these results suggest that CIII in *A. castellanii* corresponds in composition to the well-described CIII of bovine, yeast and plant mitochondria.

Table 3
A. castellanii CIII subunits and CIII-associated proteins.

Protein	Genome	WM	BN	Euk.	Bact.	Amoeb.
CIII subunits						
Core1	N	+	+	+	+[a]	+
Core2	N	+	+	+	+[a]	+
Cob	M	+	+	+	+	+
Isp	N	+	+	+	+	+
Cytc1	N	+	+	+	+	+
Qrc6	N	+	+	+	–	+
Qcr7	N	+	+	+	–	+
Qcr8	N	+	+	+	–	+
Qcr9	N	+	+	+	–	+
Qcr10	N	+	+	+	–	+
CIII assembly proteins						
Bcs1	N	+	–	+	+[b]	+
Cbp3	N	+	–	+	+	+

See Table 1 for details. Protein sequences for all entries, including delineation of identified peptides, are available in Supplemental File 1. BN, proteomic analysis of complex isolated by BN-PAGE.
[a]The Core1 and Core2 proteins have bacterial homologs (M16 family proteases), but are not components of bacterial CIII.
[b]While AAA^+ ATPase homologs are encoded by bacteria, it is doubtful that they are orthologs.

3.3.3. Evolution of CIII Core proteins

In certain land plants, CIII Core proteins constitute the mitochondrial processing peptidase responsible for proteolytic cleavage of mitochondrial targeting sequences [46]. In contrast, in *Saccharomyces cerevisiae* [47] and animals [48], an evolutionarily related, heterodimeric mitochondrial processing peptidase (MPP), comprising MPPα and MPPβ (homologous to Core2 and Core1 proteins, respectively), is present in the mitochondrial matrix. An intermediate scenario is seen in *Neurospora crassa* [49] and *D. discoideum* [50], as the sole isoform of Core1/MPPβ exists in both the membrane and the matrix, while MPPα is found only in the matrix (and a separate Core2 is associated with CIII). In animals and *S. cerevisiae*, the catalytic matrix-localized MPPβ subunit possesses the Zn-binding His-x-x-Glu-x-His-x~76-Glu motif characteristic of all active pitrilysin protease family members, whereas the CIII-associated Core1 does not. Conversely, the CIII-associated Core1/MPPβ protein in plant CIII has retained this motif [51].

Similar to what is observed in plant mitochondria and *D. discoideum*, the CIII-associated Core1 protein is the only isoform of Core1/MPPβ present in *A. castellanii* (i.e., a separate, distinct MPPβ protein could not be identified in the *A. castellanii* nuclear genome or EST databases). Furthermore, *A. castellanii* Core1/MPPβ has the characteristic pitrilysin motif described above, suggesting that it likely possesses mitochondrial processing peptidase activity. Two separate proteins of the Core2/MPPα family are encoded in *A. castellanii*, as is the case in *D. discoideum*; however, only Core2 was detected in the BN-PAGE CIII fraction. Core2 appears to be by far the more abundant of the two proteins, as its MS/MS ion scores were among the highest in the entire proteome (strongly detected in each of four fractions), whereas only a single high-scoring peptide representing the other homolog was detected in one of the four separate fractions tested (SWM). It is not clear why there are two distinct Core2/MPPα family proteins in *A. castellanii*, although a fraction of the Core1/MPPβ protein of *A. castellanii* may be associated with Core2 (in CIII), while another fraction associates with the minor MPPα family protein in the mitochondrial matrix, as reported in *D. discoideum*. CIII-associated Core1/MPPβ and Core2/MPPα were detected in abundance in both the MPE and SPE fractions by proteomic analyses, although ion scores were higher for MPE fractions.

A maximum likelihood phylogenetic reconstruction of Core1/MPPβ proteins suggests that relatively recent gene duplications or losses within established eukaryotic lineages likely account for the duality of the Core1/MPPβ family, as opposed to an ancient gene duplication early in eukaryotic evolution (Supplemental Fig. 1). Specifically, the human, yeast and *T. thermophila* Core1 proteins are more closely related to MPPβ homologs from the same species than to other Core1 proteins from other species. Thus, it may be that independent gene duplications of the Core subunits resulted in separate matrix processing peptidases and the inactivation of the Core subunits in certain lineages (such as animals, fungi and ciliates) whereas the CIII Core1/MPPβ protein retained enzymatic activity in other eukaryotes (plants and possibly *A. castellanii*).

3.3.4. CIII assembly proteins

In yeast, the assembly of CIII is aided by several factors [52], among which Cbp3 and Bcs1 are conserved widely among eukaryotes. Homologs of Bcs1 and Cbp3 were identified by proteomic analysis in *A. castellanii* mitochondria, although none was detected in isolated CIII after BN-PAGE.

3.4. Complex IV (cytochrome c:O_2 oxidoreductase; CIV)

Mitochondria have inherited 3 subunits of CIV (Cox1–3) from the protomitochondrial endosymbiont; however, the mitochondrial complex has acquired additional subunits [13,53–55]. Cox1, a large, multipass membrane-spanning protein, is encoded in mtDNA (but see [56]), whereas Cox2 and Cox3 are specified by either mtDNA or nuDNA, depending on the organism [5]. In *A. castellanii*, Cox1-3 are all encoded in mtDNA; atypically, however, Cox1 and Cox2 are transcribed from a single continuous ORF [31], as is also the case in the related amoebozoan, *D. discoideum* [57]. However, mature Cox1 and Cox2 appear to exist as separate proteins in *A. castellanii* mitochondria [58].

3.4.1. Analysis of CIV size and higher order structure in A. castellanii

The majority of active *A. castellanii* CIV exists in a complex of ~360 kDa (Fig. 1), suggesting that CIV may be predominantly dimeric under the conditions used for BN-PAGE. The band exhibiting the majority of cytochrome oxidase activity was quite broad (Fig. 1); notably, activity assays performed after BN-PAGE using a minigel setup demonstrated the presence of two similarly sized, enzymatically active bands (Supplemental Fig. 2A), possibly explaining the breadth of this band in the large-format gel. Similarly, plant mitochondrial CIV exists as two distinct (350- and 280-kDa) complexes after BN-PAGE, with the larger complex including an additional subunit homologous to Cox6b [13,59]. Our results are in contrast to a previous report on *A. castellanii* CIV after BN-PAGE [39], which detected enzymatic activity in a smaller, ~160-kDa band. What accounts for the differences between the two studies is unclear, although the fact that mitochondria were harvested from stationary phase cells in the prior report may partially explain this discrepancy.

3.4.2. CIV subunit composition

CIV was detected by proteomic analysis in several different bands isolated from BN-PAGE, although it was not the sole, or even dominant, species in any of them, suggesting that the complex may not be stable under the conditions employed. All CIV subunits identified after BN-PAGE were present in the broad ~360-kDa band (Table 4; Supplemental File 1A-4). Peptides from all mtDNA-encoded proteins, Cox1/2 and Cox3, were detected after BN-PAGE, as well as from the nuDNA-encoded proteins Cox1-c [56], Cox4 and Cox5b. In addition, a protein homologous to Cox7c (designated Cox7c-1) was identified after BN-PAGE, although another isoform (Cox7c-2), 69% identical in amino acid sequence (Supplemental File 1C-4), was not detected after BN-PAGE or in whole mitochondria. A homolog of Cox6a and two homologs of Cox6b – one considerably more similar to Cox6b from other eukaryotes – were detected in the analysis of whole mitochondria; however, none was identified by BN-PAGE. Cox6b was not found in an analysis of CIV from *D. discoideum* [53], suggesting that this subunit may dissociate readily from the complex during isolation.

A predicted 8.7-kDa protein, not seen in whole mitochondria, was identified after BN-PAGE. HMMER searches suggest that this protein may be a homolog of Cox7a. Lastly, an ~11-kDa protein lacking assignable BLASTp homologs was identified in the ~360-kDa complex. This protein was the third highest hit in HMMER searches of the *A. castellanii* mitochondrial protein dataset when a profile including only amoebozoan Cox6c homologs was employed. Like Cox6c homologs from other eukaryotes, it contains a predicted ~20-amino acid transmembrane helix. Multiple alignments demonstrate some similarity to amoebozoan Cox6c; however, the similarity to Cox6c from other eukaryotes is very weak. In sum, our analyses suggest that *A. castellanii* CIV likely consists of ≥10 subunits (Table 4).

3.4.3. CIV assembly proteins

In yeast, assembly of CIV is mediated by at least 20 factors (many of which appear to be yeast-specific) involved in translational regulation, heme *a* synthesis, and insertion of copper/heme [60]. Proteomic analysis of *A. castellanii* mitochondria and bioinformatic searches have identified proteins involved in the maturation of copper centers, including Cox11, Cox17, Cox19, Cox23, Cmc1 and Sco1 (Table 4, Supplemental File 1B-4, 1C-4). Cox15, but not Cox10 – both required for the synthesis of heme *a* – was identified in whole mitochondria.

3.4.4. Cox1/2 protein structure

Our analysis provides further support for the conclusion that mature Cox1 and Cox2 do not exist as a fusion protein in *A. castellanii* mitochondria [58]. Specifically, combined 1D SDS-PAGE and MS/MS experiments indicate that two individual proteins likely exist, because distinct peptide

Table 4
A. castellanii CIV subunits and CIV-associated proteins.

Protein	Genome	WM	BN	Euk.	Bact.	Amoeb.
CIV subunits						
Cox1/2	M	+	+	+	+	+
Cox3	M	+	+	+	+	+
Cox1-c	N	+	+	+	+[a]	+[a]
Cox4	N	+	+	+	–	+
Cox5b	N	+	+	+	–	+
Cox6a	N	+	–	+	–	+
Cox6b-1	N	+	–	+	–	+
Cox6b-2	N	+	–	+	–	+
Cox6c[b]	N	+	+	+	–	+
Cox7a[b]	N	–	+	+	–	-
Cox7c-1	N	+	+	+	–	+
Cox7c-2	N	–	–	+	–	+
CIV-associated proteins						
Cox11	N	+	–	+	+	+
Cox17	N	+	–	+	–	+
Cox19	N	+	–	+	–	+
Cox23	N	+	–	+	–	+
Cmc1	N	+	–	+	–	+
Sco1	N	+	–	+	+	+
Pet100	N	+	–	+	–	+
Cox10	N	–	–	+	+	+
Cox15	N	+	–	+	+	+
Shy1	N	+	–	+	+	+
Pet191	N	–	–	+	–	+

See Table 1 for details. Protein sequences for all entries, including delineation of identified peptides, are available in Supplemental File 1. BN, proteomic analysis of complex isolated by BN-PAGE.
[a]CoxI-c is a nuDNA-encoded protein homologous to the C-terminal portion of Cox1. *D. discoideum* also encodes a homolog known to be a component of CIV [53].
[b]The putative Cox6c and Cox7a homologs were annotated based on HMMER 3.0 profile searches, and their assignment is therefore less certain than in the case of other CIV proteins.

populations corresponding to predicted Cox1 or Cox2 protein sequences were found in different regions of the gel after SDS-PAGE (Fig. 2). For instance, in an MPE fraction, Cox1-specific peptides were detected in gel slices 16–22 (~58 kDa → 100 kDa), whereas Cox2-specific peptides were only found in slice 9 (~31 kDa). In addition, a targeted Mascot search uncovered a semitryptic peptide that may correspond to the mature, processed N-terminus of Cox2. The detection of this peptide suggests that a 16-residue N-terminal sequence, 'MVSLSVLFIFYDSLLC', is proteolytically removed (assuming that Cox2 starts with M541 of the Cox1/2 ORF), consistent with the removal of a 15-residue N-terminal portion of yeast Cox2 during its maturation [61].

Proteomic results answer other outstanding questions about the structure of mature Cox2. As described [58], the *A. castellanii* Cox2 sequence contains several apparent 'insertions' that predict that the mature protein should be considerably longer than Cox2 from other species (333 vs. 236 amino acids in *A. castellanii* and *S. cerevisiae*, respectively); however, *A. castellanii* and yeast Cox2 co-migrate in SDS-PAGE, raising the possibility that the insertion sequences are not a part of the mature Cox2. We detected peptides from both of these Cox2 'insert' regions (Fig. 2), indicating that mature *A. castellanii* Cox2 does retain these extra sequences but evidently migrates anomalously faster than would be expected during SDS-PAGE.

3.5. Complex V (F_1Fo ATP synthase; CV)

Bacterial (*E. coli*) CV consists of 8 different proteins, with the α, β, γ, δ and ε subunits constituting the F_1 sector while a, b and c comprise F_o [62]. In general, the subunits of the F_1 head sector are highly conserved across eukaryotes and few additional subunits have been added; conversely, bacterial F_o subunit homologs are more variable at the sequence level; moreover, the base and stator domains of F_o have gained novel subunits. As in other respiratory complexes, some eukaryote-specific subunits (e.g., Atpd = Atp7) are conserved across Eucarya. Others are reported to be more limited in distribution, leading to variable numbers of CV subunits in eukaryotes, ranging from ≥9 in jakobid protists [63], 11–13 in plants [12,59], 16 in *C. reinhardtii* [15], 18 in yeast [64,65], 16 in humans [66] to ≥20 in *T. thermophila* [19] and 22 in *Trypanosoma brucei* [16].

3.5.1. ATP synthase size and higher order structure in *A. castellanii*

Under the conditions employed here, the major, enzymatically active form of *A. castellanii* CV is >1 MDa in size (Fig. 1). Typically in eukaryotes, monomeric CV is ~550–600 kDa; thus, the >1-MDa band is likely a dimer, which appears quite stable, even at relatively high detergent concentrations. Dimeric ATP synthase, which appears to be very abundant, as judged by profiles from 1D BN-PAGE (Fig. 1), 2D BN/SDS-PAGE [24] and protein ion scores, is the only observable enzymatically active form at concentrations as high as 2% (w:v) DDM; at 5% DDM, much of the complex breaks down into a smaller, ~820-kDa variant with weak ATPase activity (Supplemental Fig. 2B).

The high stability of the *A. castellanii* CV dimer is in marked contrast to that of the yeast and bovine dimer, which must be prepared under gentle conditions, employing mild delipidating detergents such as digitonin [65,67]. The monomers that comprise these dimeric complexes in *S. cerevisiae* are held together by dimer-specific subunits, including Atpe, Atpg, Atpi/j and Atpk [65,68]. Conversely, the stable dimeric nature of *A. castellanii* CV is reminiscent of mitochondrial ATP synthase from the green algae *C. reinhardtii* and *Polytomella* sp. [15]. In *Polytomella* sp., an ~1600-kDa dimeric CV is the predominant enzymatically active form, dissociating only upon heat treatment or detergent concentrations ≥10% DDM [69]. Notably, CV from these chlorophyte algae contains 8 novel subunits that play a role in dimerization of the complex [15,70].

3.5.2. Analysis of ATP synthase composition

The subunit composition of CV (Table 5; Supplemental File 1A-5) was investigated by proteomic analysis of in-gel-digested dimeric CV obtained via 1D BN-PAGE (Table 5, Supplemental File 1A-5) and various other CV isoforms detected by BN-PAGE after separation in a linear 10–40% sucrose gradient (Supplemental Table 1).

3.5.2.1. F_1 subunits. All of the expected F_1 subunits (α, β, γ, δ and ε subunits) were present in dimeric *A. castellanii* CV (Table 5, Supplemental File 1A-5, 1B-5). A smaller, low-abundance subcomplex, isolated via BN-PAGE after linear sucrose gradient centrifugation, also contained the same subunits (Supplemental Table 1) and likely corresponds to the dissociated F_1 head sector, which appears similar to those in other eukaryotes. These results suggest that most, if not all, of the other identified subunits are associated with the F_o base or stator stalk. However, no isolated F_o sector was detected in BN gels, so this inference needs experimental confirmation.

3.5.2.2. F_o subunits. Proteomic analysis revealed several of the expected F_o subunits, both mtDNA-encoded and nuDNA-encoded, in dimeric *A. castellanii* CV (Table 5, Supplemental File 1A-5). Moreover, proteomic analysis provided strong support for previous suggestions that certain mtDNA-encoded ORFs are constituents of CV. In particular, OrfB (Orf142) and Orf25 (Orf124) were both confidently identified as components of CV, in good agreement with previous analyses, which suggested that they are homologous to Atp8 and Atp4, respectively [5,12]. No standard tryptic peptides from mtDNA-encoded subunit a (Atp6) were found in any BN-PAGE-isolated CV isoforms, although a single semitryptic peptide was confidently detected, and one acceptable tryptic peptide was identified in the analysis of whole mitochondria.

3.5.2.3. 'Hypothetical' CV proteins. An Atp7 (subunit d) profile search using HMMER identified a predicted 56-kDa CV component, having no obvious matches in the NCBI nr database (including in *D. discoideum*),

MINR**LLNNLTSFFTDNR**WLFSTNHKDIGTLYLIFGGFSGIIGTIFSMIIRLELAAPGSQILSGNSQLYNV
IITAHAFVMIFFFVMPVMIGGFGNWFVPLMIGAPDMAFPRLNNISFWLLPPSLFLLLCSSLVEFGAGTGW
TVYPPLSSIVAHSGGSVDLAIFSLHLAGISSLLGAINFITTIFNMRVPGLSMHKLPLFVWSVLITAFLLL
FSLPVLAGAITMLLTDRNFNTSFFDPSGGGDPILYQHLFWFFGHPEVYILILPAFGIVSQIIGTFSNKSI
FGYIGMVYAMLSIAVLGFIVWAHHMYTVGLDVDTRAYFTAATMMIAVPTGIKIFSWIATLWGGQIVRKTP
LLFVIGFLILFTLGGLTGIVLSNAGLDIMLHDTYYVVAHFHYVLSMGAVFAFFAGFYYWFWKISGYTYNE
MYGNVHFWLMFIGVNLTFFPMHFVGLAGMPRRIPDYPDNYYYWNILSSFGSIISSVSVIVFFYLIYLAFN
NNNTPKLIK**LVHSIFAPYINTLSKNLLTFASIK**STSDSSFFKFSKFFIFF**MVSLS**VLFIFYDSLLC**LNDH**
TNSWKIGFQDPTTPIAYGIIKLHDHILFFLAVILFVVGYLLLSTYKKFYYGSLNNDLPESKR**ISLFDTLI**
NTYKENLSFNVTNRTYNINHGTTIEIIWTILPAFILLFIAVPSFALLYAMDEIIDPVLTVKVIGHQWYWS
YEYSDYSVVYSNR**MLDYDSIDR**FAAMEMMYKGMGYLKDRSLLSYLYIPMVIPETTIK**FDSYMIHEAELNL**
GDLRLLK**TDMPLFLPK**NTHIR**LLITSSDVLHSWAVPSFGVK**VDAVPGR**LNQTSLYLK**NTGTFYGQCSELC
GVNHAFMPIEVYVVNPVYFYNYVYIYFKNFNLI

Fig. 2. Proteomic-based evidence for separate Cox1 and Cox2 proteins in *A. castellanii* mitochondria. Identified peptides are inferred from a Mascot search of mtDNA-encoded proteins from the MPE fraction (SDS-PAGE). Bold red text marks confidently identified peptides from gel slices 18–22 that appear to be derived from mature Cox1 (~58 kDa→100 kDa; presumably the protein runs aberrantly due to its highly hydrophobic nature). Bold blue text delineates peptides identified from gel slice 9 that seemingly correspond to Cox2 (between 27 and 34.6 kDa). These results suggest that the mature C-terminus of Cox1 is located near the 'MVSLS' (bold, underlined) believed to be the pre-processed N-terminus of Cox2. The identification of a Cox2 semitryptic peptide ('LNDHTNSWK'; yellow highlight) suggests that the N-terminus of *A. castellanii* Cox2 is processed, as reported in yeast [61]. Peptides from the 'insert' regions of *A. castellanii* Cox2, described in [58], were confidently detected: **ISLFDTLINTYK**, and **ENLSFNVTNR** from one insert and **MLDYDSIDR** from the other. These data suggest that these 'inserts' are likely to be retained as a part of the mature Cox2 protein and that the latter may migrate anomalously fast.

Table 5
A. castellanii CV subunits and CV-associated proteins.

Protein	Genome	WM	BN	Euk	Bact.	Amoeb.
CV proteins						
$F_1\alpha$ (Atp1)	M	+	+	+	+	+
$F_1\beta$ (Atp2)	N	+	+	+	+	+
$F_1\gamma$ (Atp3)	N	+	+	+	+	+
$F_1\varepsilon$ (Atp15)	N	+	+	+	-	+
$F_1\delta$ (Atp16)	N	+	+	+	+	+
F_o a (Atp6)	M	+	+	+	+	+
F_o b (Orf25; Atp4)	M	+	+	+	+	+
F_o c (Atp9)	M	+	+	+	+	+
F_o OSCP (Atp5)	N	+	+	+	+	+
F_o A6L (OrfB; Atp8)	M	+	+	+	+[a]	+
Atpd[b] (Atp7)	N	+	+	+	-	+
Atpg[b] (Atp20)	N	+	+	+	-	+
Atpi/j[b] (Atp18)	N	+	+	+	-	+
Atpf (Atp17)	N	+	+	+	-	+
15510[c]	N	+	+	-	-	-
31[c]	N	+	+	-	-	-
24711[c]	N	+	+	-	-	-
MDH[d]	N	+	+	+	+	+
CV-associated proteins						
INH1	N	+	-	+	-	+
Atp10	N	+	-	+	-	+
Atp11	N	+	-	+	-	+
Atp12	N	+	-	+	+	+
Atp23	N	+	-	+	-	+
NCA2	N	+	-	+	-	+

See Table 1 for details. Protein sequences for all entries, including delineation of identified peptides, are available in Supplemental File 1. BN, proteomic analysis of complex isolated by BN-PAGE.
[a]BLAST searches using protist Atp8/A6L as query retrieve α-proteobacterial ATP synthase B′, a stator stalk subunit not present in *E. coli* CV.
[b]These subunits were annotated via HMMER 3.0 profile searches.
[c]These proteins do not have identifiable homologs in other organisms. Names/numbers reflect the EST contig numbers to facilitate retrieval from the proteome database.
[d]Malate dehydrogenase was found to be associated with CV in *A. castellanii*. MDH homologs are present in other eukaryotes and bacteria, but have not been reported to be associated with CV in these cases.

as a likely Atp7 subunit. Most notably, a short C-terminal region of the putative *A. castellanii* Atp7 is similar to homologs from other eukaryotes (Fig. 3A). The putative *A. castellanii* Atp7 protein is quite divergent and substantially larger than other identified subunit d homologs, all of which (including Atp7 from *D. discoideum*) are predicted to be ~20 kDa in size. Notably, Atp7 is not the only *A. castellanii* CV subunit that is considerably larger than its homologs; for instance, the OSCP (Atp5) subunit and the otherwise highly conserved F_1 β subunit (Atp2; Supplemental Fig. 3) have C-terminal extensions of ~165 and ~140 amino acids, respectively. In each case, the C-terminal extension is predicted to contain additional helical components. Unlike the case of subunit d, the OSCP and β subunits of other amoebozoons also appear to have C-terminal extensions, as does the β subunit of *C. reinhardtii*.

Other apparently *A. castellanii*-specific CV subunits were identified by proteomic analysis; in some of these cases, putative homology inferences have been made after detailed bioinformatic searches, although 3 proteins remain without annotation. A number of the identified subunits appear to be related to proteins characterized as CV dimer-specific proteins in yeast. For instance, profile HMM similarity searches identified a predicted 10.6-kDa protein as a homolog of yeast Atpi/j (Atp18), important in the stepwise dimerization and/or oligomerization of CV in yeast [68]. HMMER searches also uncovered a previously unidentified homology: specifically, Atpi/j is related to the 6-kDa plant ATP synthase subunit [71], which has multiple protist homologs as well. This conclusion is supported by a multiple protein alignment, which demonstrates regions conserved between the plant/protist and yeast proteins (Fig. 3B) and indicates that Atpi/j is likely a very ancient component of CV in eukaryotes.

In HMMER searches, another *A. castellanii* CV subunit that could not be annotated by conventional BLASTp retrieves subunit g (=Atp20), also a protein identified in yeast CV as dimer-specific [65]. The *A. castellanii* protein is similar in size to the yeast and human homologs of subunit g. We detected Atp20 homologs in a wide variety of eukaryotic groups, including *D. discoideum*, although the latter homolog is more highly conserved than its *A. castellanii* counterpart. Although BLAST similarity scores are low, multiple alignments demonstrate similarity in the C-terminal region of the protein (data not shown). Taken together, these results suggest that *A. castellanii* likely encodes homologs of certain proteins required for dimerization of yeast ATP synthase,

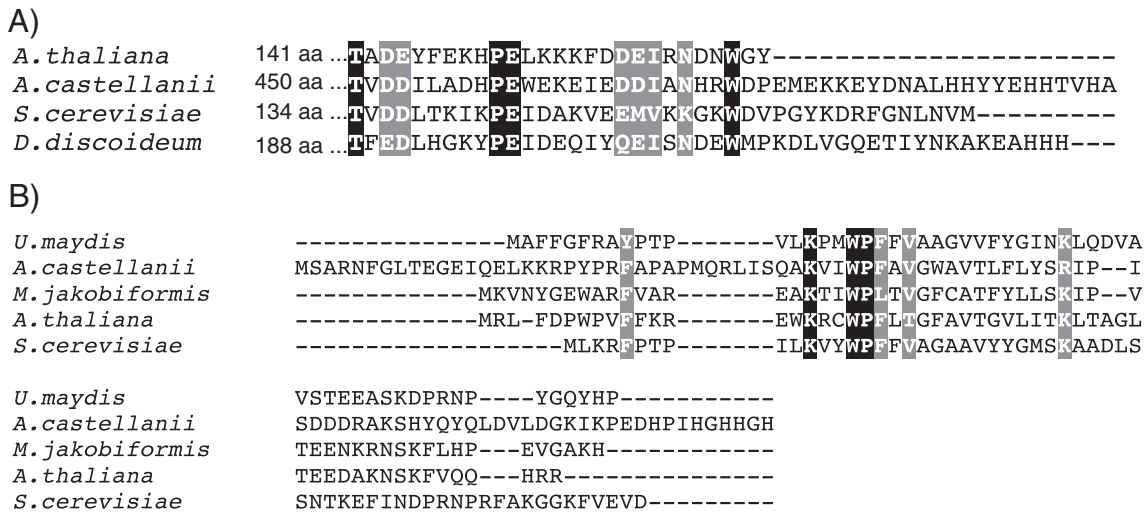

Fig. 3. *A. castellanii* CV proteins annotated via HMMER 3.0 searches. A) Alignment of the C-terminal region of an expanded and divergent *A. castellanii* Atpd homolog with the corresponding region of Atpd from other eukaryotes. Numbers refer to the N-terminal amino acids omitted from the alignment. B) An *A. castellanii* CV protein is homologous to yeast Atpi/j (Atp18) and a 6-kDa component of plant CV. A multiple protein alignment of putative Atpi/j homologs from several species provides evidence that Atpi/j was an early addition to mitochondrial CV. Black and gray shading represent 100% and ≥75% similar sites, respectively.

proteins that are likely widespread among eukaryotes. In addition to fungi, dimerization of CV has been described in animals [67], plants [59], green algae [15,69,72] and other protists [16,19], suggesting that the dimerization of ATP synthase may be functionally important, as has been reported in yeast [73].

Unexpectedly, malate dehydrogenase (MDH) – the terminal enzyme of the TCA cycle – was found to be associated with CV in *A. castellanii*. Initially, we attributed this result to contamination of dimeric CV by an abundant mitochondrial protein, as in the case of other *A. castellanii* respiratory complexes isolated by BN-PAGE. However, MDH was identified in several distinct variants of CV; MDH ion scores were consistently among the highest for CV, usually only eclipsed by the α and β subunits; few other contaminating proteins were found in proteomic analyses of isolated CV; and only one suspected contaminant was found in more than one CV variant (Supplemental Table 1). However, MDH was not detected in the subcomplex thought to represent the soluble F_1 sector, suggesting that MDH (along with other novel proteins) may be associated with the F_o sector. To our knowledge, an association of MDH with CV has not been reported in other organisms.

In sum, our results suggest that CV of *A. castellanii* is predominantly dimeric and comprises ~18 subunits, adding up to a molecular weight in excess of 1 MDa. The stable interaction of CV monomers, even at relatively high detergent concentrations, is reminiscent of CV isolated from *C. reinhardtii* and *Polytomella* sp. Also, like green algal CV, but to a lesser extent, subunits of the stator stalk appear to be especially unusual [15]. As the stator stalk serves a primarily structural role – it does not contain any subunits directly involved in catalysis – strict conservation of protein sequence may not be critical for CV function. Whether CV dimerization in *A. castellanii* is achieved by interaction between novel and divergent stator stalk elements, as in green algae, or via the putative dimer-specific subunits that are also found in other eukaryotes, remains to be investigated.

3.5.3. CV assembly proteins

Proteomic analyses of *A. castellanii* mitochondria have identified factors putatively involved in the expression, regulation and assembly of CV [64]. These factors include homologs of yeast NCA2, which plays a role in the expression of mtDNA-encoded F_o subunits 6 (Atpa) and 8 (A6L/OrfB); INH1 (IF_1 in mammals), the endogenous F_1F_o ATP synthase inhibitor; and a number of assembly proteins/chaperones, specifically Atp10, Atp11 and Atp12 and Atp23 (Table 5).

3.6. Branched respiratory chain

In contrast to mammalian mitochondria, ETCs of fungi, plants and protists are often branched [74,75], containing external and internal rotenone-insensitive NADH:ubiquinone oxidoreductases (facing the cytoplasm and matrix, respectively) and a cyanide-insensitive alternative oxidase (AOX), which accepts electrons from ubiquinol and reduces O_2 (normally catalyzed by CIV).

In *A. castellanii* mitochondria, we identified 3 distinct proteins that are homologous to rotenone-insensitive NADH dehydrogenase. The inferred molecular weights of the preproteins are ~53, 66 and 70 kDa, and all are predicted to have N-terminal mTPs. BLAST analyses could not provide significant insight into the precise function of any given homolog (i.e., whether it is an external or internal NADH dehydrogenase).

An AOX protein was identified in this study by proteomic analysis. *A. castellanii* AOX has been described previously [75,76]; two isoforms, A and B, are encoded by genes that differ only by an insertion/deletion of 12 nucleotides in the portion of exon 1 that encodes the mTP [77]. Proteomic analysis did not identify any peptides corresponding to the mTP portion of AOX, therefore we were unable to determine whether only one or both isoforms were present. Additionally, our proteomic analysis failed to reveal an association of AOX with CIII, as reported elsewhere [39], although one peptide from AOX was identified in the CIV-enriched ~360-kDa band.

4. Conclusions

Comparative genomic analyses aimed at uncovering conserved ETC subunits have been, and will continue to be, very important in furthering our understanding of the composition and evolution of ETC complexes, along with their dedicated assembly systems. Nonetheless, these approaches are limited in that standard similarity searches often fail to identify novel subunits, as well as certain small and divergent but phylogenetically conserved subunits. More sensitive similarity searches may uncover putative homologs; however, in the absence of supporting biochemical evidence, these assignments must be treated with caution. Conversely, proteomic analyses of isolated ETC complexes and whole mitochondria or submitochondrial fractions, in conjunction with sensitive and targeted bioinformatic analyses, greatly increases our confidence in homology assignments inferred for divergent subunits. In our comprehensive characterization of the *A. castellanii* ETC, the first for a member of the eukaryotic supergroup Amoebozoa, this combined

proteomic and bioinformatic approach has allowed us to identify most of the phylogenetically conserved ETC subunits and assembly factors, providing evidence for a relatively conservative composition. Nevertheless, ETC complex isolation in conjunction with proteomic analysis and coupled with profile-based similarity searches, allowed us to identify several novel and conserved ETC subunits that would not have been confidently identified otherwise, including MWFE and ASHI of CI, Qcr10 of CIII, Cox7a of CIV, along with subunits d, g and i/j of CV. Our results emphasize the importance of biochemical enrichments in unraveling protist mitochondrial evolution, as the candidate status of a bioinformatically identified homolog of divergent ETC subunits is greatly strengthened by the detection of that protein in the cognate ETC complex.

BN-PAGE and/or proteomic analyses can provide other valuable information about ETC complexes. With respect to ultrastructure, our BN-PAGE analyses indicate that the majority of enzymatically active CV likely exists as a stable dimer or multimer, similar to CV in chlorophyte algae and certain other protists. Additional biochemical examinations of CV dimerization in *A. castellanii*, and comparisons to stable dimeric ATP synthases from other organisms, may yield further insights into the mechanisms and role of CV dimerization in general.

Finally, our proteomic analyses have provided evidence supporting unusual primary protein structures inferred from the corresponding gene sequences. For instance, we have identified peptides from a long C-terminal extension on the otherwise highly conserved β and OSCP subunits of CV and 'insert' sequences from Cox2, demonstrating that these unusual features persist in the mature protein products. Likewise, our data confirm that Cox1 and Cox2 exist as separate protein species in *A. castellanii* mitochondria, even though the two proteins are expressed from a single continuous ORF in *A. castellanii* mtDNA.

Supplementary data to this article can be found online at http://dx.doi.org/10.1016/j.bbabio.2012.06.005.

Acknowledgements

The authors thank Drs. David Spencer and Murray Schnare for helpful discussions. Operating grant support to M.W.G. from the Canadian Institutes of Health Research (MOP-4124) as well as funding from the Tula Foundation is gratefully acknowledged. R.M.R.G. was supported by a Predoctoral Scholarship from the Killam Trusts.

References

[1] M.W. Gray, G. Burger, B.F. Lang, Mitochondrial evolution, Science 283 (1999) 1476–1481.
[2] M.W. Gray, B.F. Lang, G. Burger, Mitochondria of protists, Annu. Rev. Genet. 38 (2004) 477–524.
[3] M.W. Gray, J.M. Archibald, Origins of mitochondria and plastids, in: R. Bock, V. Knoop (Eds.), Genomics of Chloroplasts and Mitochondria, Springer, Dordrecht, 2012, pp. 1–30.
[4] P. Mitchell, J. Moyle, Chemiosmotic hypothesis of oxidative phosphorylation, Nature 213 (1967) 137–139.
[5] M.W. Gray, B.F. Lang, R. Cedergren, G.B. Golding, C. Lemieux, D. Sankoff, M. Turmel, N. Brossard, E. Delage, T.G. Littlejohn, I. Plante, P. Rioux, D. Saint-Louis, Y. Zhu, G. Burger, Genome structure and gene content in protist mitochondrial DNAs, Nucleic Acids Res. 26 (1998) 865–878.
[6] S. Berry, Endosymbiosis and the design of eukaryotic electron transport, Biochim. Biophys. Acta 1606 (2003) 57–72.
[7] T. Gabaldón, D. Rainey, M.A. Huynen, Tracing the evolution of a large protein complex in the eukaryotes, NADH:ubiquinone oxidoreductase (Complex I), J. Mol. Biol. 348 (2005) 857–870.
[8] U. Brandt, Energy converting NADH:quinone oxidoreductase (complex I), Annu. Rev. Biochem. 75 (2006) 69–92.
[9] J. Carroll, I.M. Fearnley, J.M. Skehel, R.J. Shannon, J. Hirst, J.E. Walker, Bovine complex I is a complex of 45 different subunits, J. Biol. Chem. 281 (2006) 32724–32727.
[10] A. Abdrakhmanova, V. Zickermann, M. Bostina, M. Radermacher, H. Schägger, S. Kerscher, U. Brandt, Subunit composition of mitochondrial complex I from the yeast *Yarrowia lipolytica*, Biochim. Biophys. Acta 1658 (2004) 148–156.
[11] J.L. Heazlewood, K.A. Howell, A.H. Millar, Mitochondrial complex I from *Arabidopsis* and rice: orthologs of mammalian and fungal components coupled with plant-specific subunits, Biochim. Biophys. Acta 1604 (2003) 159–169.
[12] J.L. Heazlewood, J. Whelan, A.H. Millar, The products of the mitochondrial *orf25* and *orfB* genes are F_O components in the plant F_1F_O ATP synthase, FEBS Lett. 540 (2003) 201–205.
[13] A.H. Millar, H. Eubel, L. Jänsch, V. Kruft, J.L. Heazlewood, H.-P. Braun, Mitochondrial cytochrome *c* oxidase and succinate dehydrogenase complexes contain plant specific subunits, Plant Mol. Biol. 56 (2004) 77–90.
[14] P. Cardol, F. Vanrobaeys, B. Devreese, J. Van Beeumen, R.F. Matagne, C. Remacle, Higher plant-like subunit composition of mitochondrial complex I from *Chlamydomonas reinhardtii*: 31 conserved components among eukaryotes, Biochim. Biophys. Acta 1658 (2004) 212–224.
[15] M. Vázquez-Acevedo, P. Cardol, A. Cano-Estrada, M. Lapaille, C. Remacle, D. González-Halphen, The mitochondrial ATP synthase of chlorophycean algae contains eight subunits of unknown origin involved in the formation of an atypical stator-stalk and in the dimerization of the complex, J. Bioenerg. Biomembr. 38 (2006) 271–282.
[16] A. Zíková, A. Schnaufer, R.A. Dalley, A.K. Panigrahi, K.D. Stuart, The F_oF_1-ATP synthase complex contains novel subunits and is essential for procyclic *Trypanosoma brucei*, PLoS Pathog. 5 (2009) e1000436.
[17] J. Morales, T. Mogi, S. Mineki, E. Takashima, R. Mineki, H. Hirawake, K. Sakamoto, S. Ōmura, K. Kita, Novel mitochondrial complex II isolated from *Trypanosoma cruzi* is composed of 12 peptides including a heterodimeric Ip subunit, J. Biol. Chem. 284 (2009) 7255–7263.
[18] P. Cardol, Mitochondrial NADH:ubiquinone oxidoreductase (complex I) in eukaryotes: A highly-conserved subunit composition highlighted by mining of protein databases, Biochim. Biophys. Acta 1807 (2011) 1390–1397.
[19] P.B. Nina, N.V. Dudkina, L.A. Kane, J.E. van Eyk, E.J. Boekema, M.W. Mather, A.B. Vaidya, Highly divergent mitochondrial ATP synthase complexes in *Tetrahymena thermophila*, PLoS Biol. 8 (2010) 1–5 (e1000418).
[20] D.G.S. Smith, R.M.R. Gawryluk, D.F. Spencer, R.E. Pearlman, K.W.M. Siu, M.W. Gray, Exploring the mitochondrial proteome of the ciliate protozoon *Tetrahymena thermophila*: direct analysis by tandem mass spectrometry, J. Mol. Biol. 374 (2007) 837–863.
[21] J.L. Heazlewood, J.S. Tonti-Filippini, A.M. Gout, D.A. Day, J. Whelan, A.H. Millar, Experimental analysis of the *Arabidopsis* mitochondrial proteome highlights signaling and regulatory components, provides assessment of targeting prediction programs, and indicates plant-specific mitochondrial proteins, Plant Cell 16 (2004) 241–256.
[22] H. Schägger, G. von Jagow, Blue native electrophoresis for isolation of membrane protein complexes in enzymatically active form, Anal. Biochem. 199 (1991) 223–231.
[23] A.J. Lohan, M.W. Gray, Analysis of 5′- or 3′-terminal tRNA editing: mitochondrial 5′ tRNA editing in *Acanthamoeba castellanii* as the exemplar, Methods Enzymol. 424 (2007) 223–242.
[24] R.M.R. Gawryluk, M.W. Gray, Evidence for an early evolutionary emergence of γ-type carbonic anhydrases as components of mitochondrial respiratory complex I, BMC Evol. Biol. 348 (2010) 857–870.
[25] J. Klodmann, S. Sunderhaus, M. Nimtz, L. Jänsch, H.-P. Braun, Internal architecture of mitochondrial complex I from *Arabidopsis thaliana*, Plant Cell 22 (2010) 797–810.
[26] E. Zerbetto, L. Vergani, F. Dabbeni-Sala, Quantification of muscle mitochondrial oxidative phosphorylation enzymes *via* histochemical staining of blue native polyacrylamide gels, Electrophoresis 18 (1997) 2059–2064.
[27] V. Méchin, C. Damerval, M. Zivy, Total protein extraction with TCA-acetone, Methods Mol. Biol. 355 (2006) 1–8.
[28] U.K. Laemmli, Cleavage of structural proteins during the assembly of the head of bacteriophage T4, Nature 227 (1970) 680–685.
[29] S. Lim, K. Chisholm, R.H. Coffin, R.D. Peters, K.I. Al-Mughrabi, G. Wang-Pruski, D.M. Pinto, Protein profiling in potato (*Solanum tuberosum* L.) leaf tissues by differential centrifugation, J. Proteome Res. 11 (2012) 2594–2601.
[30] E.A. O'Brien, L.B. Koski, Y. Zhang, L. Yang, E. Wang, M.W. Gray, G. Burger, B.F. Lang, TBestDB: a taxonomically broad database of expressed sequence tags (ESTs), Nucleic Acids Res. 35 (2007) D445–D451.
[31] G. Burger, I. Plante, K.M. Lonergan, M.W. Gray, The mitochondrial DNA of the amoeboid protozoon. *Acanthamoeba castellanii*: complete sequence, gene content and genome organization, J. Mol. Biol. 245 (1995) 522–537.
[32] M. Stanke, S. Waack, Gene prediction with a hidden Markov model and a new intron submodel, Bioinformatics 19 (2003) ii215–ii225.
[33] L. Kreppel, P. Fey, P. Gaudet, E. Just, W.A. Kibbe, R.L. Chisholm, A.R. Kimmel, dictyBase: a new *Dictyostelium discoideum* genome database, Nucleic Acids Res. 32 (2004) D332–D333.
[34] S.F. Altschul, T.L. Madden, A.A. Schäffer, J. Zhang, Z. Zhang, W. Miller, D.J. Lipman, Gapped BLAST and PSI-BLAST: a new generation of protein database search programs, Nucleic Acids Res. 25 (1997) 3389–3402.
[35] S.R. Eddy, Profile hidden Markov models, Bioinformatics 14 (1998) 755–763.
[36] M. Terashima, M. Specht, B. Naumann, M. Hippler, Characterizing the anaerobic response of *Chlamydomonas reinhardtii* by quantitative proteomics, Mol. Cell. Proteomics 9 (2010) 1514–1532.
[37] A. Stamatakis, RAxML-VI-HPC: maximum likelihood-based phylogenetic analyses with thousands of taxa and mixed models, Bioinformatics 22 (2006) 2688–2690.
[38] C.-y. Yip, M.E. Harbour, K. Jayawardena, I.M. Fearnley, L.A. Sazanov, Evolution of respiratory complex I. "Supernumerary" subunits are present in the α-proteobacterial enzyme, J. Biol. Chem. 286 (2011) 5023–5033.
[39] R. Navet, W. Jarmuszkiewicz, P. Douette, C.M. Sluse-Goffart, F.E. Sluse, Mitochondrial respiratory chain complex patterns from *Acanthamoeba castellanii* and *Lycopersicon esculentum*: comparative analysis by BN-PAGE and evidence of protein–protein interaction between alternative oxidase and complex III, J. Bioenerg. Biomembr. 36 (2004) 471–479.

[40] E.H. Meyer, J.L. Heazlewood, A.H. Millar, Mitochondrial acyl carrier proteins in *Arabidopsis thaliana* are predominantly soluble matrix proteins and none can be confirmed as subunits of respiratory complex I, Plant Mol. Biol. 64 (2007) 319–327.
[41] H.R. Bridges, I.M. Fearnley, J. Hirst, The subunit composition of mitochondrial NADH:ubiquinone oxidoreductase (complex I) from *Pichia pastoris*, Mol. Cell. Proteomics 9 (2010) 2318–2326.
[42] M. McKenzie, M.T. Ryan, Assembly factors of human mitochondrial complex I and their defects in disease, IUBMB Life 62 (2010) 497–502.
[43] R.M.R. Gawryluk, M.W. Gray, A split and rearranged nuclear gene encoding the iron–sulfur subunit of mitochondrial succinate dehydrogenase in Euglenozoa, BMC Res. Notes 2 (2009) 16.
[44] C. Lange, C. Hunte, Crystal structure of the yeast cytochrome bc_1 complex with its bound substrate cytochrome *c*, Proc. Natl. Acad. Sci. U. S. A. 99 (2002) 2800–2805.
[45] S. Iwata, J.W. Lee, K. Okada, J.K. Lee, M. Iwata, B. Rasmussen, T.A. Link, S. Ramaswamy, B.K. Jap, Complete structure of the 11-subunit bovine mitochondrial cytochrome bc_1 complex, Science 281 (1998) 64–71.
[46] H.-P. Braun, M. Emmermann, V. Kruft, M. Bödicker, U.K. Schmitz, The general mitochondrial processing peptidase from wheat is integrated into the cytochrome bc_1-complex of the respiratory chain, Planta 195 (1995) 396–402.
[47] M. Yang, R.E. Jensen, M.P. Yaffe, W. Oppliger, G. Schatz, Import of proteins into yeast mitochondria: the purified matrix processing protease contains two subunits which are encoded by the nuclear *MAS1* and *MAS2* genes, EMBO J. 7 (1988) 2605–2612.
[48] W.-J. Ou, A. Ito, H. Okazaki, T. Omura, Purification and characterization of a processing protease from rat liver mitochondria, EMBO J. 8 (1989) 2605–2612.
[49] G. Hawlitschek, H. Schneider, B. Schmidt, M. Tropschug, F.-U. Hartl, W. Neupert, Mitochondrial protein import: identification of processing peptidase and of PEP, a processing enhancing protein, Cell 53 (1988) 795–806.
[50] K. Nagayama, S. Itono, T. Yoshida, S.-i. Ishiguro, H. Ochiai, T. Ohmachi, Antisense RNA inhibition of the b subunit of the *Dictyostelium discoideum* mitochondrial processing peptidase induces the expression of mitochondrial proteins, Biosci. Biotechnol. Biochem. 72 (2008) 1836–1846.
[51] H.-P. Braun, U.K. Schmitz, Are the 'core' proteins of the mitochondrial bc_1 complex evolutionary relics of a processing protease? Trends Biochem. Sci. 20 (1995) 171–175.
[52] V. Zara, L. Conte, B.L. Trumpower, Biogenesis of the yeast cytochrome bc_1 complex, Biochim. Biophys. Acta 1793 (2009) 89–96.
[53] R. Bisson, G. Schiavo, Two different forms of cytochrome *c* oxidase can be purified from the slime mold *Dictyostelium discoideum*, J. Biol. Chem. 261 (1986) 4373–4376.
[54] J.W. Taanman, R.A. Capaldi, Purification of yeast cytochrome *c* oxidase with a subunit composition resembling the mammalian enzyme, J. Biol. Chem. 267 (1992) 22481–22485.
[55] T. Tsukihara, H. Aoyama, E. Yamashita, T. Tomizaki, H. Yamaguchi, K. Shinzawa-Itoh, R. Nakashima, R. Yaono, S. Yoshikawa, The whole structure of the 13-subunit oxidized cytochrome c oxidase at 2.8 Å, Science 272 (1996) 1136–1144.
[56] R.M.R. Gawryluk, M.W. Gray, An ancient fission of mitochondrial *cox1*, Mol. Biol. Evol. 27 (2010) 7–10.
[57] R. Pellizzari, C. Anjard, R. Bisson, Subunits I and II of *Dictyostelium* cytochrome *c* oxidase are specified by a single open reading frame transcribed into a large polycistronic RNA, Biochim. Biophys. Acta 1320 (1997) 1–7.
[58] K.M. Lonergan, M.W. Gray, Expression of a continuous open reading frame encoding subunits 1 and 2 of cytochrome *c* oxidase in the mitochondrial DNA of *Acanthamoeba castellanii*, J. Mol. Biol. 257 (1996) 1019–1030.
[59] H. Eubel, L. Jänsch, H.-P. Braun, New insights into the respiratory chain of plant mitochondria. Supercomplexes and a unique composition of complex II, Plant Physiol. 133 (2003) 274–286.
[60] F. Fontanesi, I.C. Soto, A. Barrientos, Cytochrome *c* oxidase biogenesis: new levels of regulation, IUBMB Life 60 (2008) 557–568.
[61] E. Pratje, G. Mannhaupt, G. Michaelis, K. Beyreuther, A nuclear mutation prevents processing of a mitochondrially encoded membrane protein in *Saccharomyces cerevisiae*, EMBO J. 2 (1983) 1049–1054.
[62] A.E. Senior, S. Nadanaciva, J. Weber, The molecular mechanism of ATP synthesis by F_1F_0-ATP synthase, Biochim. Biophys. Acta 1553 (2002) 188–211.
[63] G. Burger, B.F. Lang, H.-P. Braun, S. Marx, The enigmatic mitochondrial ORF *ymf39* codes for ATP synthase chain b, Nucleic Acids Res. 31 (2003) 2353–2360.
[64] S.H. Ackerman, A. Tzagoloff, Function, structure, and biogenesis of mitochondrial ATP synthase, in: M. Kivie (Ed.), Prog Nucleic Acid Res Mol Biol, Academic Press, 2005, pp. 95–133.
[65] I. Arnold, K. Pfeiffer, W. Neupert, R.A. Stuart, H. Schägger, Yeast mitochondrial F_1F_0-ATP synthase exists as a dimer: identification of three dimer-specific subunits, EMBO J. 17 (1998) 7170–7178.
[66] R. Aggeler, J. Coons, S.W. Taylor, S.S. Ghosh, J.J. Garcia, R.A. Capaldi, M.F. Marusich, A functionally active human F_1F_0 ATPase can be purified by immunocapture from heart tissue and fibroblast cell lines. Subunit structure and activity studies, J. Biol. Chem. 277 (2002) 33906–33912.
[67] F. Minauro-Sanmiguel, S. Wilkens, J.J. García, Structure of dimeric mitochondrial ATP synthase: novel F_0 bridging features and the structural basis of mitochondrial cristae biogenesis, Proc. Natl. Acad. Sci. U. S. A. 102 (2005) 12356–12358.
[68] K. Wagner, I. Perschil, C.D. Fichter, M. van der Laan, Stepwise assembly of dimeric F_1F_o-ATP synthase in mitochondria involves the small F_o-subunits k and i, Mol. Biol. Cell 21 (2010) 1494–1504.
[69] A. Villavicencio-Queijeiro, M. Vázquez-Acevedo, A. Cano-Estrada, M. Zarco-Zavala, M. Tuena de Gómez, J. Mignaco, M. Freire, H. Scofano, D. Foguel, P. Cardol, C. Remacle, D. González-Halphen, The fully-active and structurally-stable form of the mitochondrial ATP synthase of *Polytomella* sp. is dimeric, J. Bioenerg. Biomembr. 41 (2009) 1–13.
[70] A. Cano-Estrada, M. Vázquez-Acevedo, A. Villavicencio-Queijeiro, F. Figueroa-Martínez, H. Miranda-Astudillo, Y. Cordeiro, J.A. Mignaco, D. Foguel, P. Cardol, M. Lapaille, C. Remacle, S. Wilkens, D. González-Halphen, Subunit–subunit interactions and overall topology of the dimeric mitochondrial ATP synthase of *Polytomella* sp., Biochim. Biophys. Acta 1797 (2010) 1439–1448.
[71] S. Liu, X. Zhang, Expression and purification of a novel rice (*Oryza sativa* L.) mitochondrial ATP synthase small subunit in *Escherichia coli*, Protein Expr. Purif. 37 (2004) 306–310.
[72] N.V. Dudkina, J. Heinemeyer, S. Sunderhaus, E.J. Boekema, H.-P. Braun, Respiratory chain supercomplexes in the plant mitochondrial membrane, Trends Plant Sci. 11 (2006) 232–240.
[73] P. Paumard, J. Vaillier, B. Coulary, J. Schaeffer, V. Soubannier, D.M. Mueller, D. Brèthes, J.-P. di Rago, J. Velours, The ATP synthase is involved in generating mitochondrial cristae morphology, EMBO J. 21 (2002) 221–230.
[74] A.G. Rasmusson, K.L. Soole, T.E. Elthon, Alternative NAD(P)H dehydrogenases of plant mitochondria, Annu. Rev. Plant Biol. 55 (2004) 23–39.
[75] W. Jarmuszkiewicz, F.E. Sluse, L. Hryniewiecka, C.M. Sluse-Goffart, Interactions between the cytochrome pathway and the alternative oxidase in isolated *Acanthamoeba castellanii* mitochondria, J. Bioenerg. Biomembr. 34 (2002) 31–40.
[76] W. Jarmuszkiewicz, A.M. Wagner, M.J. Wagner, L. Hryniewiecka, Immunological identification of the alternative oxidase of *Acanthamoeba castellanii* mitochondria, FEBS Lett. 411 (1997) 110–114.
[77] F.L. Henriquez, J. McBride, S.J. Campbell, T. Ramos, P.R. Ingram, F. Roberts, S. Tinney, C.W. Roberts, *Acanthamoeba* alternative oxidase genes: identification, characterisation and potential as antimicrobial targets, Int. J. Parasitol. 39 (2009) 1417–1424.